

THE UNIVERSITY OF MANITOBA

POSTNATAL DEVELOPMENT OF THE CUNEATE NUCLEUS IN EUTHYROID AND
HYPOTHYROID RATS--AN ULTRASTRUCTURAL STUDY

by

SAMUEL DAVID

A THESIS

SUBMITTED TO THE FACULTY OF GRADUATE STUDIES IN PARTIAL
FULFILMENT OF THE REQUIREMENTS FOR THE DEGREE

DOCTOR OF PHILOSOPHY

DEPARTMENT OF ANATOMY

FACULTY OF MEDICINE

WINNIPEG, MANITOBA

FEBRUARY 1979

POSTNATAL DEVELOPMENT OF THE CUNEATE NUCLEUS IN EUTHYROID AND
HYPOTHYROID RATS--AN ULTRASTRUCTURAL STUDY

BY

SAMUEL DAVID

A dissertation submitted to the Faculty of Graduate Studies of
the University of Manitoba in partial fulfillment of the requirements
of the degree of

DOCTOR OF PHILOSOPHY

© 1979

Permission has been granted to the LIBRARY OF THE UNIVER-
SITY OF MANITOBA to lend or sell copies of this dissertation, to
the NATIONAL LIBRARY OF CANADA to microfilm this
dissertation and to lend or sell copies of the film, and UNIVERSITY
MICROFILMS to publish an abstract of this dissertation.

The author reserves other publication rights, and neither the
dissertation nor extensive extracts from it may be printed or other-
wise reproduced without the author's written permission.

Dedicated with love and respect
to my parents
who taught me to value the pursuit
of knowledge above everything else

"Let us not delude ourselves by dreaming that great achievements are imminent. Let us eschew 'breakthroughs' lest we incur frustrating breakdowns. Let us strive for equanimity in our quest for the 'truth', remembering that whatever we call 'truth' is tentative and subject to revision as our verifiable knowledge increases, and that 'even unwelcomed truth is better than cherished error'. Let us patiently support the long-term scientific endeavor. It would be brash indeed to think that the secrets evolved over billions of years will yield overnight even with the most generous of financial backing."

Chauncey D. Leake. JAMA 193: 54-58, 1965

ACKNOWLEDGEMENTS

I wish to express my sincere appreciation to my advisor, Dr. E.J.H. Nathaniel, for his invaluable assistance, advice and criticism in the preparation of this thesis.

I would also like to thank all the members of the Anatomy Department for their warmth and friendship.

My special thanks to Dr. D.R. Nathaniel, Mrs. Ertrice Eddy and Ms. Aley Thomas for the warm interaction I have enjoyed in the laboratory. To Mr. Paul Perumal for sharing his exceptional technical knowledge, Mr. Roy Simpson for his superb photographic assistance in rephotographing the master prints, and Miss Roslyn Hoad for her cheerfulness and immense patience in the typing of this manuscript.

Thanks is also due to Dr. T.V.N. Persaud, Chairman of the Department of Anatomy, for the opportunity of working in the department.

Above all I am grateful to the Medical Research Council of Canada for a Studentship which was awarded during the tenure of this research.

ABSTRACT

The postnatal ultrastructural differentiation of neuronal, glial, and vascular components of the cuneate nucleus were studied in normal rats with the light and electron microscope (Part I). This formed the basis for comparable studies in neonatally induced hypothyroidism (Part II).

PART I - Sprague-Dawley rats were sacrificed by perfusion with Karnovsky's fixative, at weekly intervals from birth to six weeks, and the region of the cuneate nucleus fixed for electron microscopy.

Neurons. Light and dark neurons were observed, the former constituting the predominant cell type. At birth light neurons displayed mild nuclear invaginations and scanty cytoplasm with few organelles. By two weeks, the cytoplasm had markedly increased containing large Nissl bodies. These neurons were characterized by somatic spines. Spherical and non-spherical neurons could be identified. At three weeks, neurons contained numerous short, lamellar arrays of endoplasmic reticulum. Between three and six weeks, there was a reduction in Nissl substance. Spherical neurons differed from non-spherical neurons in the amount of Nissl substance and number of axo-somatic synapses. The dark neurons increased from birth to three weeks and decreased thereafter both in number and electron density. Postnatal development was accompanied by a series of nuclear and cytoplasmic changes within dark neurons. Four types of intranuclear inclusions, viz., rodlets, fibrillar lattices, microtubules and membranous bodies were observed.

Glial cells. These were classified as: (i) Glioblasts - mitotic, small and large glioblasts and glial precursors; (ii) Astrocytic series - early, immature, and mature; (iii) Oligodendrocytic series - light, medium and dark; and (iv) Microglia - immature and mature. Mitotic glioblasts were considered to give rise to small glioblasts containing primarily polyribosomes. Patchy chromatin characterized large glioblasts. Glial precursors possessed a large nucleus with masses of heterochromatin and cytoplasm resembling either an astrocyte or an oligodendrocyte. Early astrocytes had a dark, irregular nucleus and numerous glycogen granules. Maturation was accompanied by an apparent decrease in nuclear invaginations, electron density, glycogen granules, and microtubules, and an increase in filaments and dense bodies. Light and medium oligodendrocytes were not seen until one week and dark oligodendrocytes until four weeks. There was a progressive reduction in size and an increase in electron density between light, medium and dark oligodendrocytes. Microglial cells possessed large masses of heterochromatin, long, stringy segments of rough endoplasmic reticulum, dense bodies and lipid droplets. Mature microglia, contained numerous microtubules and well-developed Golgi complexes.

Blood vessels. Quantitative studies revealed a doubling of blood vessel profiles between one and three weeks. At early stages, vessels displayed slit-like lumina and thick endothelial cells resting on a basal lamina of uneven thickness, and surrounded by large, clear astrocytic processes. With maturation the endothelial cells attenuated with a concomitant increase in lumen size. The basal lamina became even in thickness and the astrocytic processes contained filaments.

PART II - Hypothyroidism was induced in newborn Sprague-Dawley rats by daily SC injections of propylthiouracil (PTU): 0.05 ml of 0.2% PTU on days 0-10; 0.1 ml of 0.2% PTU on days 11-20; 0.1 ml of 0.4% PTU on days 21-30; and 0.2 ml of 0.4% PTU on days 30-42. Controls received equivolumens physiological saline. Animals were sacrificed as in Part I.

Neurons. The sequence of maturational changes generally resembled those of the controls, however a number of differences were noted. Some light neurons at seven days displayed dilations of perinuclear space, rough endoplasmic reticulum, Golgi complexes and mitochondria. A few degenerating neurons were noted. Three changes were observed in neurites in all age groups: (a) large accumulations of glycogen in presynaptic terminals, (b) clear vacuoles, and (c) numerous mitochondria and lamellar dense bodies within reactive axons. Marked mitochondrial swelling was apparent by day 14. Aberrant myelination of three kinds were observed beyond one week: (a) portions of oligodendroglial cytoplasm trapped between myelin lamellae, (b) single myelin sheath enclosing multiple processes, and (c) collapsed and redundant myelin. Signs of intramyelinic vacuolization were evident from three weeks onwards. At four weeks the perikarya and myelinated axons contained glycogen. At six weeks, large, clear cytoplasmic vacuoles appeared associated with a drastic reduction in cytoplasmic organelles. Presynaptic terminals showed a 50% reduction of mitochondrial numbers. Dark neurons remained similar to controls.

Glial cells. Apart from the 12 varieties of glial cells seen in controls, reactive-astrocytes, oligodendrocytes and microglia were observed. The glioblasts remained largely unaltered. The glycogen content was reduced in early astrocytes whereas mature astrocytes displayed

an increase in glycogen, nuclear invaginations, and a decrease in filaments. Reactive astrocytes, contained numerous filaments and glycogen, and surrounded degenerating material. Light oligodendrocytes showed striking mitochondrial swelling, whereas medium oligodendrocytes displayed swellings of mitochondria and rough endoplasmic reticulum. The rough endoplasmic reticulum was often poorly developed in medium and dark oligodendrocytes. Phagocytic activity was observed in reactive oligodendrocytes and microglia. Immature microglia showed hypertrophy, whereas mature microglia contained increased heterogeneous dense bodies.

Blood vessels. There occurred a significant reduction in blood vessel profiles. The earliest change consisted of pericytic hypertrophy. By three weeks, large, pale, inclusion-laden cells appeared between pericytes and basal lamina. After four weeks, astrocytic end-feet were often edematous and contained glycogen granules.

TABLE OF CONTENTS

Chapter	Page
1. INTRODUCTION	1
2. AN OVERVIEW OF THE DORSAL COLUMN NUCLEI	6
2.1. INTRODUCTION	6
2.2. CYTOARCHITECTONICS	7
2.3. AFFERENT CONNECTIONS	8
2.3.1. Ascending Afferents	8
2.3.2. Descending Afferents	10
2.4. EFFERENT CONNECTIONS	11
3. MATERIALS AND METHODS	12
3.1. PART I - NORMAL	12
3.1.1. Animals	12
3.1.2. Perfusion Techniques	12
3.1.3. Removal of Tissue	12
3.1.4. Fixation and Embedding	13
3.1.5. Preparation of Solutions	14
3.1.6. Light Microscopy	14
3.1.7. Electron Microscopy	15
3.2. PART II - HYPOTHYROID EXPERIMENT	15
3.2.1. Animals	15
3.2.2. Treatment	16
3.2.3. Statistical Analysis	16

4.	NEURONS	20
4.1.	LITERATURE REVIEW	20
4.1.1.	Light Microscopy of Cuneate Neurons	20
4.1.2.	Ultrastructure of Cuneate Neurons	24
4.1.3.	Neuronal Cytodifferentiation	26
4.1.3.1.	Nuclear Changes During Cyto- differentiation	28
4.1.3.2.	Cytoplasmic Changes During Cyto- differentiation	32
4.1.3.2.1.	Endoplasmic Reticulum	32
4.1.3.2.2.	Golgi Complex	34
4.1.3.2.3.	Microtubules and Microfilaments	35
4.1.3.2.4.	Mitochondria	38
4.1.3.2.5.	Centrioles and Cilia	40
4.2.	OBSERVATIONS	41
4.2.1.	Light Neurons	42
4.2.2.	Dark Neurons	47
4.2.3.	Intranuclear Inclusions	48
4.2.4.	Cilia	49
4.3.	DISCUSSION	50
4.4.	SUMMARY	60
5.	GLIAL CELLS	95
5.1.	LITERATURE REVIEW	95
5.1.1.	Introduction	95
5.1.2.	Glioblasts	96
5.1.3.	Cells of the Astrocytic Series	99

5.1.3.1. Early Cell Forms of the Astrocytic Series	99
5.1.3.2. Mature Astrocytes	102
5.1.4. Cells of the Oligodendrocytic Series	103
5.1.4.1. Early Cell Forms of the Oligodendrocytic Series	103
5.1.4.2. Mature Oligodendrocytes	105
5.1.5. Microglia	106
5.2. OBSERVATIONS	110
5.2.1. Glioblasts	110
5.2.1.1. Mitotic Glioblasts	110
5.2.1.2. Small Glioblasts	111
5.2.1.3. Large Glioblasts	111
5.2.1.4. Glial Precursors	112
5.2.2. Astrocytic Series	112
5.2.2.1. Early Astrocytes	112
5.2.2.2. Immature Astrocytes	113
5.2.2.3. Mature Astrocytes	113
5.2.3. Oligodendrocytic Series	114
5.2.3.1. Light Oligodendrocytes	114
5.2.3.2. Medium Oligodendrocytes	115
5.2.3.3. Dark Oligodendrocytes	116
5.2.4. Microglia	116
5.2.4.1. Immature Microglia	116
5.2.4.2. Mature Microglia	117

5.3.	DISCUSSION	117
5.4.	SUMMARY	124
6.	BLOOD VESSELS	166
6.1.	LITERATURE REVIEW	166
6.2.	OBSERVATIONS	170
6.2.1.	Light Microscopy Studies	170
6.2.2.	Electron Microscope Studies	170
6.3.	DISCUSSION	174
6.4.	SUMMARY	177
 <u>PART II - HYPOTHYROID</u>		
7.	LITERATURE REVIEW	198
8.	OBSERVATIONS	205
8.1.	GENERAL	205
8.2.	NEURONS	205
8.2.1.	Light Neurons	205
8.2.2.	Dark Neurons	212
8.2.3.	Intranuclear Inclusions	213
8.3.	GLIAL CELLS	213
8.3.1.	Glioblasts	213
8.3.2.	Astrocytic Series	214
8.3.2.1.	Early Astrocytes	214
8.3.2.2.	Immature Astrocytes	215
8.3.2.3.	Mature Astrocytes	215
8.3.2.4.	Reactive Astrocytes	216
8.3.3.	Oligodendrocytic Series	217
8.3.3.1.	Light Oligodendrocytes	217
8.3.3.2.	Medium Oligodendrocytes	217

8.3.3.3. Dark Oligodendrocytes	218
8.3.3.4. Reactive Oligodendrocytes	218
8.3.4. Microglia	219
8.3.4.1. Immature Microglia	219
8.3.4.2. Mature Microglia	219
8.3.4.3. Reactive Microglia	219
8.4. BLOOD VESSELS	220
8.4.1. Light Microscopy	220
8.4.2. Electron Microscopy	220
9. DISCUSSION	224
9.1. NEURONS	224
9.2. GLIAL CELLS	235
9.3. BLOOD VESSELS	240
10. SUMMARY	242
10.1. NEURONS	242
10.2. GLIAL CELLS	243
10.3. BLOOD VESSELS	244
11. CONCLUSIONS	246
APPENDIX	339
BIBLIOGRAPHY	341

TABLE OF ILLUSTRATIONS

Figures		Page
1	Diagrammatic and Somatotopic Representation of DCN	5
2	Thyroid Gland H. & E.	17
3-18	EM of Neurons Normal Rats	63-94
19-37	EM of Glial Cells Normal Rat	127-164
38	Scheme of gliogenesis	165
39	Graph of Blood Vessel Density, Normal Rats	171
40-48	EM of Blood Vessels Normal Rats	179-196
49	Graph of Body Weight Changes	206
50-71	EM of Neurons Hypothyroid Rats	248-291
72-87	EM of Glial Cells Hypothyroid Rats	293-324
88	Graph of Blood Vessel Density, Hypothyroid Rats	221
89-94	EM of Blood Vessels Hypothyroid Rats	326-337

1. INTRODUCTION.

The relationship between congenital hypothyroidism and arrested brain development in humans was observed as early as the sixteenth century by Paracelsus (cited by Smith et al., 1957). Since then a number of studies have clearly documented the association between congenital hypothyroidism, cretinism, and mental retardation (Wilkins, 1938; Lewis, 1939; Radwin et al., 1949; Smith et al., 1957; Eayrs, 1966). In their study of 79 cases of severe cretinism, Smith et al., (1957) found 85% with I.Q.'s. of less than 90, including 41% with I.Q.'s. of 50 and below. Other signs of neurological impairment that have also been associated with this condition are spasticity, incoordination, tremors, increased deep-tendon reflexes, shuffling gait, perceptual deficits, and speech defects such as aphasia or perseveration. The electroencephalogram has also been shown to display abnormal low frequency discharges (Ross and Schwab, 1939). Some of the other clinical signs include, stunted body growth, thickened hair shafts, epiphyseal dysgenesis, poor muscle tone, and lethargy (Smith et al., 1957; Wilkins, 1962). More recently Rosman et al. (1972) reported a case of an 18-month old cretin with a 46% reduction in brain weight, as well as reductions in size of the gyri and neuronal numbers throughout the cortex.

Such insults to the nervous system observed in congenital hypothyroidism is in contrast to the predominantly non-neurologic symptoms in acquired hypothyroidism occurring in later childhood and adulthood

(myxedema). The neurologic deficits in the human cretins, correlate well with the rapid period of brain development, which occurs during the late fetal period and through the first two postnatal years.

The effects of thyroid hormone and the lack of it on the developing nervous system has been studied extensively under experimental conditions in the rat. The rat has been used largely because at birth it is both behaviourally and neurologically immature, with neuronal, and glial differentiation and growth occurring predominantly in the postnatal period (Himwich, 1962), with the peak of brain growth occurring at about the tenth postnatal day (Davison and Dobbing, 1968). The rat therefore serves as a very useful extrauterine 'fetal' model to study the effects of experimentally induced neonatal hypothyroidism on the developing nervous system.

Most investigations into the effects of neonatal hypothyroidism on the central nervous system have examined the cerebral and cerebellar cortices at the light microscopic level. The only detailed electron microscopic study is that of Lu and Brown (1977b), who examined the neurons in the developing rat caudate nucleus.

The cuneate nucleus receives spinal afferents as well as afferents from the cerebral cortex (Valverde, 1969), reticular formation (Sotgiu and Marguelli, 1976) and caudate nucleus (Jabbur et al., 1977). The cuneate neurons are also influenced by intrinsic lateral inhibitory and recurrent inhibitory circuits (Eccles, 1973). The sensory input via the dorsal column fibers is therefore modulated and refined to varying degrees in the dorsal column nuclei, e.g., cuneate neurons are inhibited during voluntary movements (Ghez and Pisa, 1972). Impairment of this modulatory effect, by alterations in the growth and development

of the dorsal column nuclei, could possibly result in faulty information processing and subsequent sensory and even motor deficits.

It was therefore felt that any impairment in the developmental morphology of the cuneate nucleus due to the effects of neonatal hypothyroidism may possibly result in altered function at this level and that some of the neurological deficits seen in this condition may not be solely due to the changes at the cortical level but may also be attributable to alterations at the subcortical levels such as the brain stem.

In order to assess the ultrastructural changes occurring within the cuneate nucleus resulting from neonatal hypothyroidism, it was essential first to establish the normal ultrastructure and patterns of developmental changes.

This study was therefore conducted in two parts. The first part was designed to establish the postnatal ultrastructural differentiation of the neuronal, glial and vascular components of the normal rat cuneate nucleus. This formed the basis for the second part, in which comparable studies were conducted in neonatally induced hypothyroidism. This study also included quantitative light microscopic estimations of blood vessel development in both the euthyroid and hypothyroid animals, using semithin (0.5 μm) araldite embedded sections.

In the interest of clarity the thesis is presented in two parts. Part I will detail the postnatal development of the cuneate nucleus in normal untreated rats, and contains chapters on neurons, glial cells and blood vessels, each of which includes sections on Literature Review, Observations, and Discussion.

In Part II, due to the limited amount of literature available on the effects of neonatal hypothyroidism on morphological changes in

the developing nervous system, it was considered best to combine all the relevant literature pertaining to neurons, glial cells and blood vessels and present them in one chapter. This will be followed by a chapter on observations, in which the neuronal, glial and vascular changes are detailed. The chapter on discussion will follow a similar pattern.

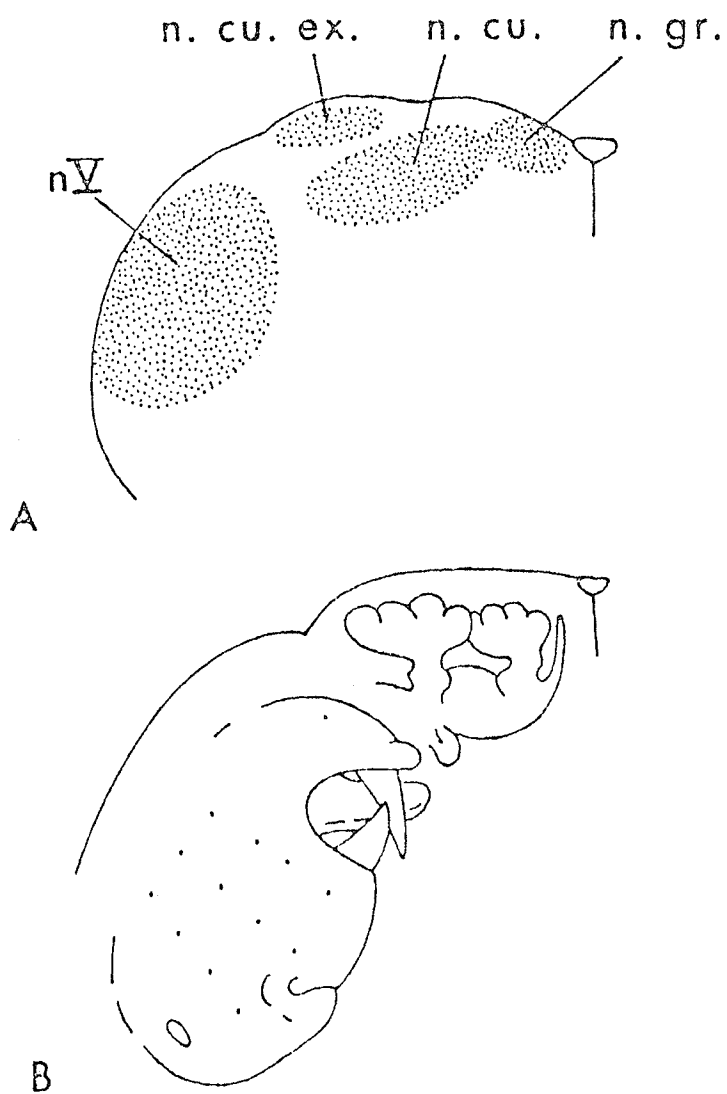


Figure 1

- A. Diagrammatic representation of the dorsal medulla at the level of the obex, showing the relative positions of the nucleus gracilis (n. gr.), nucleus cuneatus (n. cu.), external cuneate nucleus (n. cu. ex.) and the trigeminal nucleus (n.V).
- B. Somatotopic representation of the rat's body surface at the level of the obex (reproduced from S.H. Ford, 1967).

2. AN OVERVIEW OF THE DORSAL COLUMN NUCLEI.

2.1. INTRODUCTION.

The cuneate nucleus is one of a group of nuclei, collectively called the dorsal column nuclei, situated in the dorsomedial portion of the medulla oblongata at the rostral end of the dorsal columns of the spinal cord. These nuclei include a medial mass of neurons constituting the gracile nucleus (nucleus of Goll, nucleus gracilis), a lateral grey mass called the cuneate nucleus (nucleus of Burdach, nucleus cuneatus medialis) and a small group of neurons situated dorso-lateral to the cuneate nucleus, known as the external cuneate nucleus (accessory cuneate nucleus, nucleus cuneatus externus or lateralis). In rodents, the dorsal column nuclei are seen to start caudally at a level slightly below the pyramidal decussation, reaching their maximum extent with the opening of the fourth ventricle at the level of the obex, and more rostrally decreasing rapidly in size to be replaced by the vestibular nuclei (Valverde, 1966). Neuroanatomical (Hand, 1966; Keller and Hand, 1970; Basbaum and Hand, 1973) and electrophysiological (Kruger, Siminoff and Witkovsky, 1961; Nord, 1967; Millar and Basbaum, 1975) studies have shown a somatotopical organization within the gracile and cuneate nuclei, with the hind limbs, tail and lower trunk represented medially (i.e., gracile nucleus), the fore limbs and upper trunk represented laterally (i.e., cuneate nucleus), with the digits and trunk represented dorsally and ventrally, respectively, within both the nuclei (Fig. 1). In addition, in some animals a separate group of neurons known as the nucleus of Bischoff is found in the midline between

the two gracile nuclei (Bischoff, 1899). The nucleus of Bischoff is believed to receive sensory information from the tail region, however this nucleus is not always present in all mammals with a well-developed tail (Welker, Johnson and Pubols, 1964).

Recent investigations have revealed a more complex organization within the dorsal column nuclei in a number of species. A dual organization consisting of differences between the rostral and caudal portions of the cuneate nucleus has been observed in a number of studies, such as cytoarchitectonic differences (Ramon y Cajal, 1909; Kuypers and Tuerk, 1964; Hand, 1966; Keller and Hand, 1970; Biedenbach, 1972; Basbaum and Hand, 1973); differences in the pattern of dorsal root projections to the cuneate nucleus (Hand, 1966; Keller and Hand, 1970; Basbaum and Hand, 1973; Berkley, 1975); in the distribution of efferent projections from the cuneate nucleus to other brain stem nuclei (Hand and Liu, 1966; Lund and Webster, 1967) and also in the pattern of termination of somatosensory cortical afferents within the cuneate nucleus (Kuypers, 1958, 1960; Kuypers and Tuerk, 1964; Weisberg and Rustioni, 1976, 1977).

2.2. CYTOARCHITECTONICS.

Cytoarchitecturally two distinct regions have been identified in the cuneate nuclei of cats and monkeys, a caudal 'cell nest' region and a rostral 'reticular' region. In the caudal 'cell nest' region, clusters of large round cells (20 μm) are grouped together in circular aggregates with a cell free centre (Kuypers and Tuerk, 1964; Hand, 1965, 1966; Keller and Hand, 1970). Very few such studies have been done on rodents, where the findings appear contradictory. Basbaum and Hand (1973) found a single population of round cells (13 μm x 13 μm) in

the caudal region to be arranged as discrete 'bricks' or 'slabs' which run through the dorsoventral extent of the cuneate nucleus. On the other hand, Valverde (1966) noted a homogeneous arrangement within the dorsal column nuclei of the rodent. In the rostral region and in the entire length of the ventral parts of the dorsal column nuclei, especially the cuneate nucleus, the arrangement of cells is 'reticular'. In this region small cells ($10\ \mu\text{m} \times 10\ \mu\text{m}$) are diffusely scattered with a few larger cells lying among them (Keller and Hand, 1970). In the rodent, numerous cell types are observed in the rostral 'reticular' region. The most common being the round ($13\ \mu\text{m} \times 12\ \mu\text{m}$), spindle-shaped ($5\ \mu\text{m} \times 25\ \mu\text{m}$) and multipolar cells ($16\ \mu\text{m} \times 10\ \mu\text{m}$), which are scattered throughout this region (Basbaum and Hand, 1973).

2.3. AFFERENT CONNECTIONS.

The cuneate nucleus receives input from ascending spinal pathways, as well as descending afferents from the cerebral cortex, and other brain stem nuclei.

2.3.1. Ascending Afferents.

(i) The major sensory input into the cuneate nucleus is via the primary sensory afferents of the fasciculus cuneatus, which run in the dorsal funiculus of the spinal cord. These are mostly collaterals of dorsal root fibers and are not believed to contain any non-myelinated axons. Only 25% of the fibers of the cuneate fascicle are estimated to reach the cuneate nucleus, the remainder terminating in the grey matter of the spinal cord above and below the point of entry of the dorsal root into the cord (Rethelyi and Szentagothai, 1973).

The fibers of the fasciculus cuneatus are principally sensitive to touch (light pressure), hair movement, vibration, and proprioception (Kruger, 1973). However, the majority of the fibers carrying proprioceptive input are distributed to the external cuneate nucleus (Cooke et al., 1971).

Degeneration studies have shown that the primary dorsal root afferents distribute along the entire length of the cuneate nucleus (Rustioni and Macchi, 1968). However, the input to the caudal 'cell nest' region is heavier with little overlap in the distribution of adjacent roots, as compared to the rostral 'reticular' region where the distribution is more diffuse (Keller and Hand, 1970; Basbaum and Hand, 1973).

(ii) An estimated 15% of the fibers in the fasciculus gracilis and cuneatus which terminate in their respective nuclei are non-primary afferents (Uddenberg, 1968; Rustioni, 1973, 1974, 1977; Rustioni and Dekker, 1974; Rustioni and Ellis, 1978). Anatomical studies indicate that these fibers originate from the cells in the ipsilateral dorsal horn laminae III and IV (Rustioni and Dekker, 1974). Their physiological properties, however, resemble those of lamina V cells, i.e., being responsive to 'noxious' stimuli (Uddenberg, 1968; Angaut-Petit, 1975), though no relay cells have so far been found in the dorsal column nuclei that are excited by noxious stimuli (Brown and Gordon, 1977). These non-primary afferents terminate only in the reticular zone, with extensive segmental overlapping (Rustioni, 1973; Rustioni and Dekker, 1974; Rustioni and Ellis, 1978).

2.3.2. Descending Afferents.

(i) Somatosensory cortical afferents. Afferents from the contralateral somatosensory cortex, largely from layer V pyramidal cells (Weisberg and Rustioni, 1976, 1977), travel in the pyramidal tracts to the dorsal column nuclei (Chambers and Liu, 1957; Kuypers and Tuerk, 1964; Valverde, 1966). After crossing at the pyramidal decussation, these fibers run rostrally to distribute to the dorsal column nuclei and adjacent reticular formation (Valverde, 1966). In the dorsal column nuclei, these fibers are preferentially distributed to the 'reticular' zone (Kuypers and Tuerk, 1964). The ascending dorsal column afferent fibers generally tend to terminate in the dorsal portion of the dorsal column nuclei whereas the descending somatosensory pyramidal fibers end in the ventral aspect (Valverde, 1966). Electrophysiologically, cortical stimulation is seen to evoke both excitatory and inhibitory effects in the dorsal column nuclei; the inhibitory effects are believed to be mediated through brain stem mechanisms at the level of the bulbar tegmentum (Levitt et al., 1964).

(ii) Other descending afferents include afferents from the ponto-medullary reticular formation (Sotgiu and Margnelli, 1976) and caudate nucleus (Jabbur, Harik and Hush, 1976), the latter exerting an inhibitory influence on primary afferent transmission at the level of the cuneate nucleus. The terminal fields of these two afferent connections are not known.

2.4. EFFERENT CONNECTIONS.

The major efferent connections from the dorsal column nuclei is via the medial lemniscus to the contralateral ventroposterolateral nucleus of the thalamus. These fibers have been shown to arise from the round cells found in the cell clusters of the dorsal column nuclei (Kuypers and Tuerk, 1964). These axons which go to make up the medial lemniscus also give off one or more recurrent collaterals which return either to the same or to adjacent cells in the dorsal column nuclei (Valverde, 1966). The rostral region of the dorsal column nuclei in addition to sending fibers to the ventroposterolateral nucleus of the thalamus, also projects extensively to other regions including the tectum, pretectum, zona incerta and posterolateral complex (Lund and Webster, 1967). Efferents to the cerebellum are believed to exist, however their exact origins and terminations have not as yet been determined (Gordon and Seed, 1960; Hand, 1965). Connections between the cuneate nucleus and the dorsal and medial accessory olivary nuclei have also been reported (Boesten and Voogd, 1975). More recently, Barton and Loewy (1977) demonstrated efferent projections to the spinal cord, terminating in the lateral cervical nucleus, and laminae I, IV and V.

3. MATERIALS AND METHODS.

3.1. PART I - NORMAL.

3.1.1. Animals.

Four litters of Sprague-Dawley rats from a highly inbred colony, were obtained from the animal care facilities of the Faculty of Dentistry, University of Manitoba. They were maintained on a standard laboratory rat diet and water ad libitum. The pups were weighed weekly and at the same time of day.

3.1.2 Perfusion Technique.

One pup from each litter was randomly picked for sacrifice at each of the following times: birth, seven, 14, 21, 28, 35 and 42 days postnatum. Pups were weighed and then anesthetized by an intraperitoneal injection of Pentobarbital, 35 mg/kg body weight.

The thoracic cavity was opened to expose the heart. The perfusate consisting of Karnovsky's fixative (1965) at pH 7.2 was administered through the left ventricle using an 18 gauge hypodermic needle, utilizing minimal pressure. Drainage being facilitated by incision of the right atrium. A total of 25 ml of fixative was used for newborn rats and between 75 and 200 ml for older animals.

3.1.3. Removal of Tissue.

Following perfusion a craniotomy was performed and the cerebellum removed to expose the IV ventricle. The obex or inferior angle of the IV ventricle was identified and three transverse cuts made through the

medulla oblongata: (i) at the level of the obex, (ii) 1-3 mm caudal to the obex, (iii) 1-3 mm rostral to the obex. The rostral and caudal segments of the medulla oblongata thus obtained, would contain the rostral and caudal portions of the cuneate nucleus, respectively.

These pieces of tissue were then placed immediately in the same fixative. They were then sectioned into transverse slices of approximately 1 mm in thickness, utilizing a razor blade. The slices were further divided into dorsal and ventral halves and the dorsal halves divided again in the midline.

3.1.4. Fixation and Embedding.

The dorsal portions of the medulla oblongata were left in Karnovsky's fixative for 2-3 hours in the refrigerator. The tissues were then rinsed several times in 0.1 M Millonig's phosphate buffer and postfixed in 1% phosphate buffered osmium tetroxide for 1½-2 hours. The tissues were subsequently processed and embedded in Araldite 502 according to the following procedure:

1. Rinse several times in phosphate buffer.
2. 50% alcohol - two changes for a total of five minutes.
3. 75% alcohol - two changes - five minutes each.
4. 95% alcohol - two changes - seven minutes each.
5. Rinse in 100% alcohol.
6. 100% alcohol - three changes - 10 minutes each.
7. Rinse in propylene oxide.
8. Propylene oxide - three changes - 10 minutes each.
9. Equal parts of propylene oxide and araldite. Leave on rotor overnight.

10. 75% araldite and 25% propylene oxide. Leave on rotor for two hours.
11. Pure araldite. Leave on rotor for one hour.
12. Flat-embed in pure araldite, in beem capsules and leave in incubator at 40-55°C for three days.

3.1.5. Preparation of Solutions.

1. To make 500 cc of Millonig's phosphate buffer:

Solution A: 2.26% $\text{NaH}_2\text{PO}_4 \cdot \text{H}_2\text{O}$

10.17 grams in 450 ml of H_2O

Solution B: 2.52% NaOH

2.52 grams in 100 ml of H_2O

Solution C: 5.40% glucose

2.70 grams in 50 ml of H_2O

Solution D: 415 ml of Solution A + 85 ml of Solution B.

Final Buffer Solution: 50 ml of Solution C + 450 ml of Solution D.

Final pH 7.3

2. To make 200 ml of Karnovsky's fixative:

Eight grams of paraformaldehyde was dissolved in 100 ml of distilled water by heating to 65°C. One normal sodium hydroxide (NaOH) was added drop by drop to the above solution until a clear solution was obtained. After bringing to room temperature, 40 cc of a 25% glutaraldehyde solution was added. Subsequently the volume was made up to 200 cc with Millonig's phosphate buffer and the pH adjusted to 7.2.

3.1.6. Light Microscopy.

The araldite embedded blocks were sectioned at 0.5 microns, with glass knives, on a Reichert ultramicrotome. Sections were mounted on glass slides, and stained with toluidine blue. The sections were